CHAPTER II

LITERATURE REVIEW

1. Characteristics of Tunicates

Tunicates are classified in the phylum Chordata, subphylum Urochordata. The most familiar tunicates are the sea squirts or ascidians (class Ascidiacea). Adult sea squirts are sedentary, filter-feeding, cylindrical or globular animals, usually attache to rocks, shells, pilings, or boat bottoms. The soft body is surrounded by a thick test, or tunic, often transparent or translucent and varying in consistency from gelatinous to leathery. The tunic, for which the tunicates are named, is secreted by the body wall of the adult animal. Tunic is composed of cellulose, an almost unique occurrence of that material in the animal kingdom. Two siphons project from the animal body as water enters the incurrent siphon on the top of the body and leaves the excurrent siphon at the side. Food particles are filtered from the water by the pharynx, which occupies most of the body, and are then passed into the digestive system. Some species reproduce by budding, resulting in the formation of colonies of sea squirts, joined at their bases by slender stalks or embedded in a slab of common tunic material. In addition, nearly all species reproduce sexually and are hermaphroditic. Variable amounts of orange pigment occur in the mantle and is clearly visible externally in living specimens. The orange color is lost in preserved material. Tunicate retains and gestates its orange eggs in the oviduct and atrium and releases the free-swimming larva, called a tadpole, from the atrium, has a muscular tail and is similar in appearance to a frog tadpole. The tadpole eventually settles and undergoes a drastic metamorphosis into the adult form (Brusca *et al.*, 2002).

The collected Thai tunicate in this work was identified by Dr. T. Nishikawa of Nagoya University Museum as *Ecteinascidia thurstoni* Herdman, 1981 and the taxa of this genus was given by Dr. P. Kott (2003) as follows.

Kingdom : Animalia
Phylum : Chordata
Subphylum : Urochorata
Class : Ascidiaces
Order : Phlebobranchia
Family : Perophoridae
Genus : Ecteinascidia
Species : *Ecteinascidia thurstoni* Herdman, 1981

2. The tetrahydroisoquinoline antitumor agents

Several well known antitumor agents from natural products are classified into the tetrahydroisoquinoline family such as lemonomycin (**52**), cyanocycline A (**53**), quinocarcin (**54**), saframycin A (**13**), renieramycin M (**16**) and ecteinascidin 743 (**1**) (Scott *et al.*, 2002). The basic structures of these compounds are structurally characterized by the presence of a tetrahydroisoquinoline ring system which fused, varied with oxidation states, substitution patterns, and additional fragments distinguish several subfamilies of natural products. Lemonomycin (quinocarcin family) is represented a unique glycosyl unit and an aldehyde hydrate, while cyanocycline A (naphthyridinomycin family) and several closely related compounds contain an oxazolidine ring system. Quinocarcin (quinocarcin family) is characterized by an anisole ring in place of the typical quinone and an attrached carboxylic acid. The saframycins are bisquinone-containing compounds with a glyoxamide side chain, of which the renieramycins manifest an angelate ester in place of the glyoxamide unit. The ecteinascidins contain a bridging thioether ring and an additional tetrahydroisoquinoline unit, as well as oxygenated aromatic rings in place of the typical quinones (Fig. 4). Among them, Et 743 displayed highly potent cytotoxic activity in nanomolar concentration and is currently undergoing in phase II/III in clinical study (Rinehart, 2000; Jimeno *et al.*, 2004; Henriquez *et al.*, 2005).

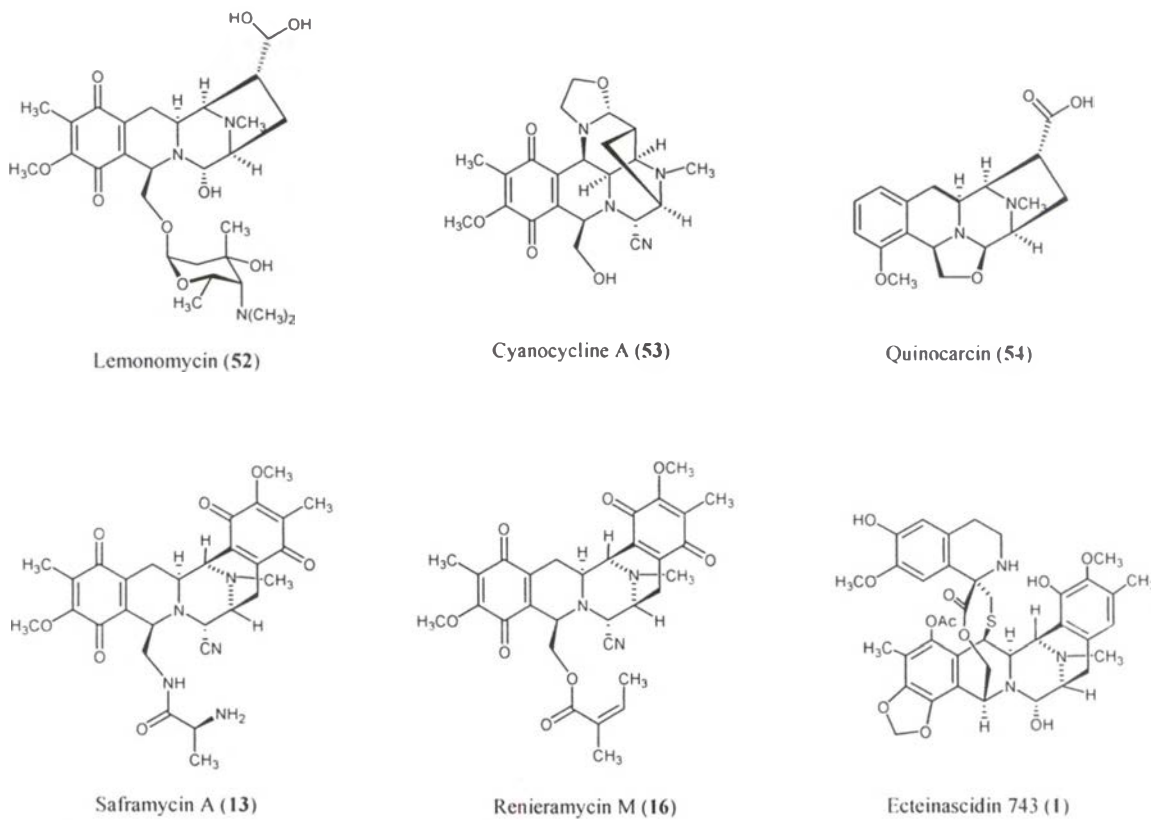

Figure 4. Structures of some other representative tetrahydroisoquinoline antitumor antibiotics.

3. Isolation and biosynthesis of ecteinascidin alkaloids

The first isolation of the ecteinascidins was reported by Rinehart *et al* (1990), and six ecteinascidins, Ets 729, 743, 745, 759A, 759B, and 770 were isolated from the Caribbean tunicate *Ecteinascidia turbinata* (Fig. 5). The structures of Ets 729 and 743 with the relative stereochemistry were elucidated later by Rinehart (1990) and Wright groups (1990). In 1992, Rinehart *et al.* reported the structures of Ets 722, 736, and 734 N^{12}-oxide, later in 1996, four putative biosynthetic precursors, Ets 594, 597, 583, and 596, were also isolated. However, all of ecteinascidins were unfortunately unstable, and it is quite difficult to obtain these natural products with a large amount for evaluating cytotoxic activity. In 2002, Suwanborirux *et al.* isolated the stable ecteinascidins, Ets 770 and 786, from the KCN-pretreated Thai tunicate, *Ecteinascidia thurstoni* Herdman, 1890 (Figure 6). The structures of ecteinascidins are summarized in Figure 1.

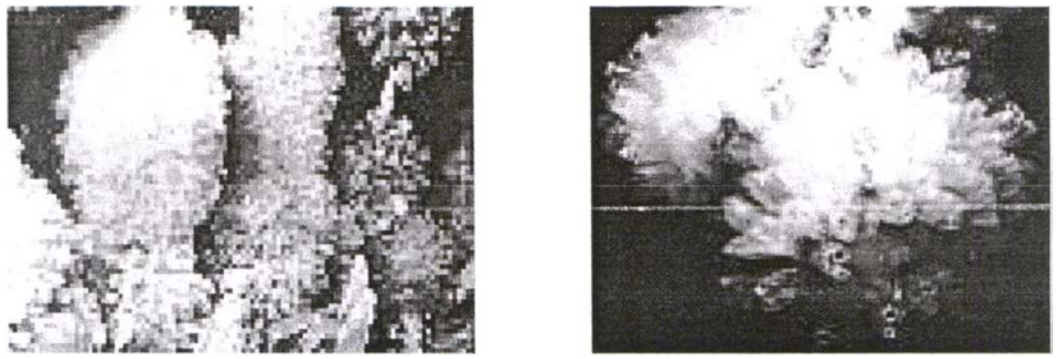

Figure 5. The picture of *Ecteinascidia turbinata* from the Caribbean tunicate

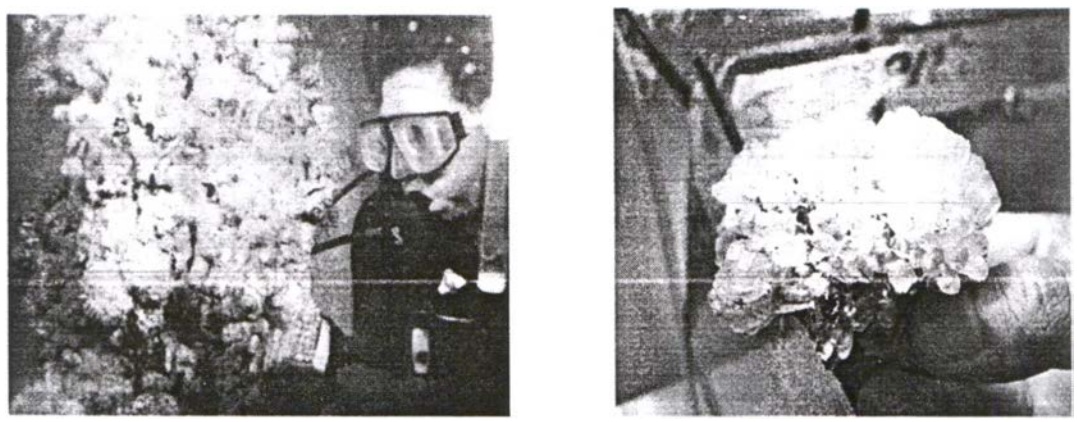

Figure 6. The picture of *Ecteinascidia thurstoni* collected from Phuket Island, Thailand

The chemical structure of most ecteinascidins is formed by a two-fused tetrahydroisoquinoline ring (*A* and *B*-subunits) which linked to another ring system, either tetrahydroisoquinoline or tetrahydro-β-carboline, forming a spiro ten-membered lactone bridge through a benzylic sulfide linkage (Sakai *et al.*, 1996). The *A*-and *B*-subunits are condensed to form a pentacyclic ring which C-1 of the C-subunit attached to C-1 and C-4 of the *B*-subunit. The *A*-and *B*-subunits basic structure of the ecteinascidin is the same as that of the saframycins and safracins, which was isolated from the cultured *Streptomyces* species (Arai *et al.*, 1980; Ikeda *et al.*, 1983, Lown *et al.*, 1983). This suggested that ecteinascidins may share the biosynthetic origin of their *A*-and *B*-subunits with those of saframycin compounds.

The biosynthetic origins of saframycin A have been elucidated by the use of isotopically labeled substrates (Figure 7) (Mikami *et al.*, 1985). It has been proposed that the central piperazine and the two quinone rings are biosynthetically derived from two molecules of tyrosine, probably through the formation of piperazine-2,5-dione from dimerization of tyrosine cyclization. while the side chain and the remaining carbons of the tetrahydroisoquinoline system derived from the dipeptide alanyl-glycine. The five methyl groups on the quinones and the *N*-methyl group derived from methylation of *S*-adenosylmethionine (SAM).

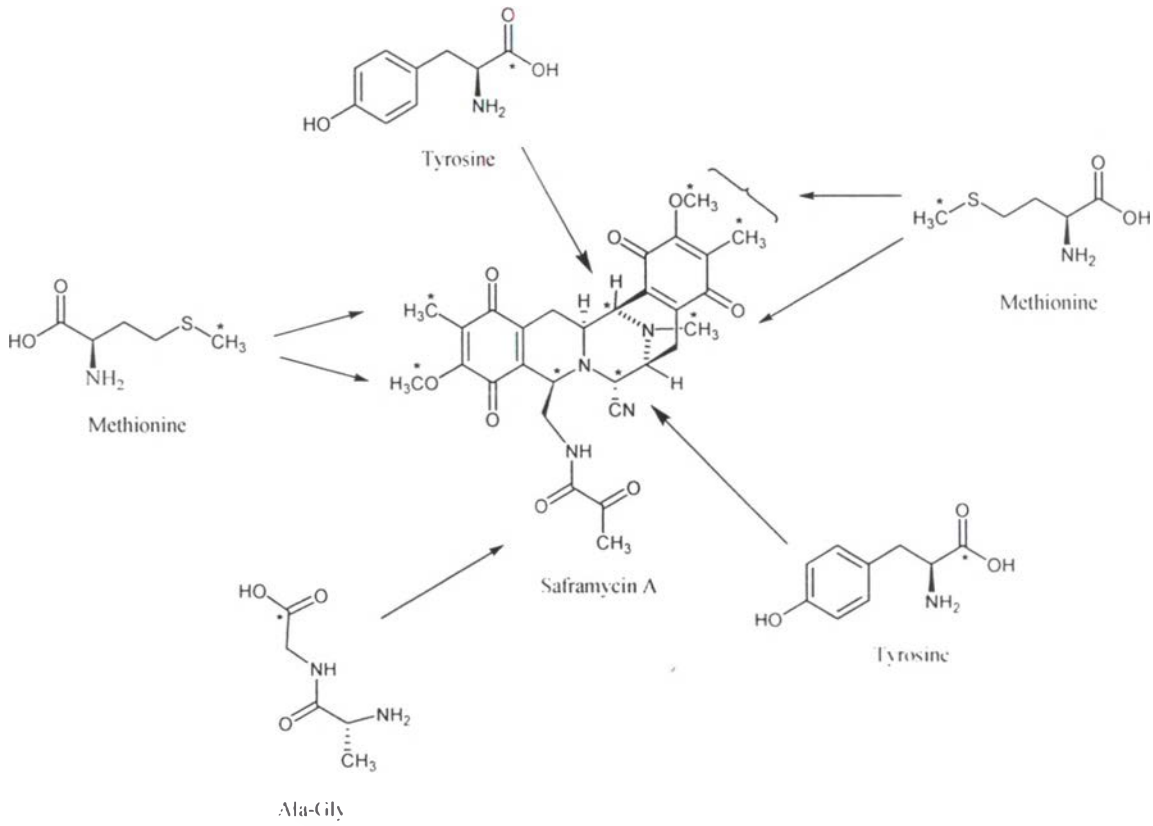

Figure 7. The proposed biosynthetic precursors of saframycin A

The biosynthetic pathway begins with the dimerization of tyrosine to form piperazine-2,5-dione **55** (Scheme 1) (Jeedigunta *et al.*, 2000). Amide reduction followed by iminium ion cyclization provides the diazabicyclic core structure **56**. Reduction of the remaining amide and incorporation of Ala-Gly produces tetrahydroisoquinoline **57**. Subsequent arene oxidation and methylation yield saframycin A (**13**). The biosynthesis of the ecteinascidins are expected to proceed through similar pathway. In 2000, Rinehart *et al.* had proposed biosynthetic pathway of ecteinascidins as shown in Scheme 2.

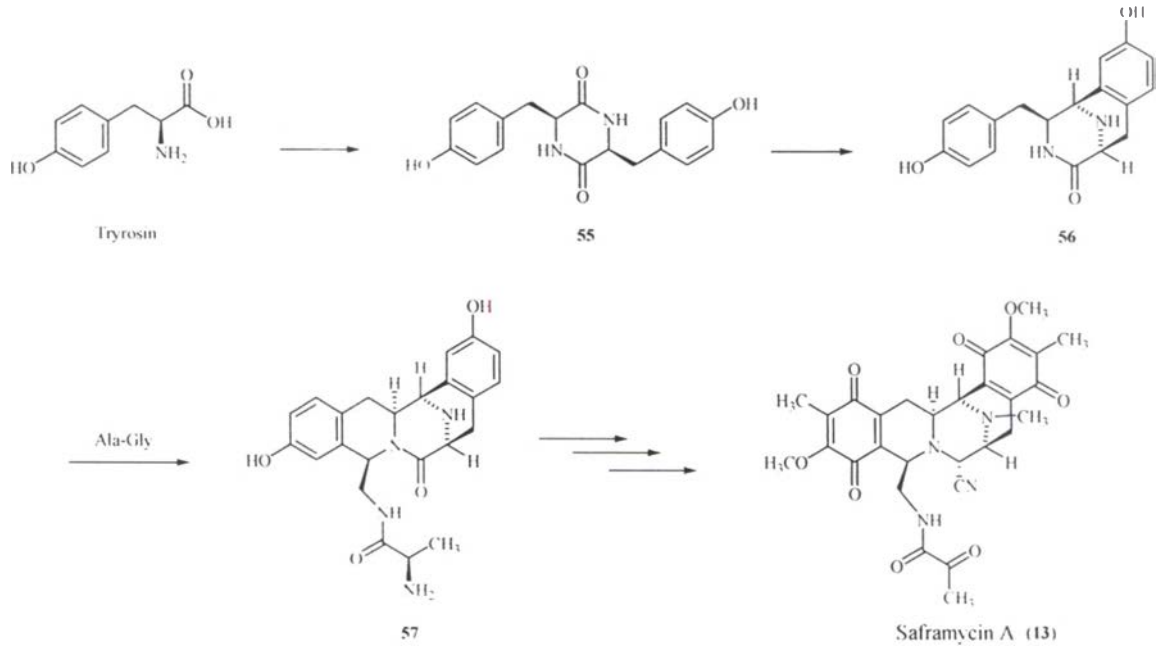

Scheme 1. Proposed biosynthetic pathway of saframycin A

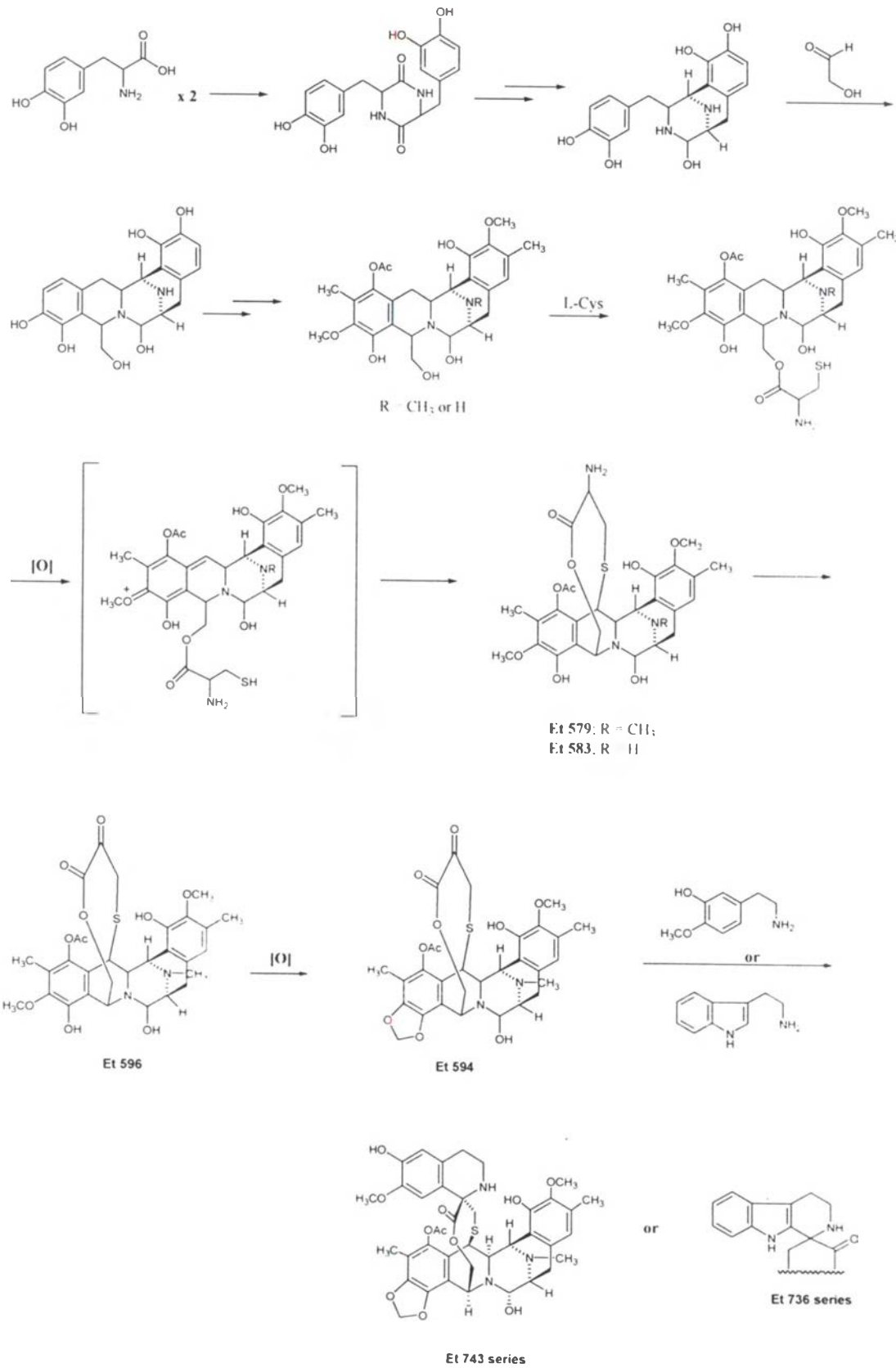

Scheme 2. Proposed biosynthetic pathway of ecteinascidins

4. Structure determination of Et 743

The core structural units in the ecteinascidin compounds were originally assigned based on Fast Atom Bombardment (FAB) technique. The basic essential unit was confirmed by the fragment ions at *m/z* 204.1027 and 218.1174 of the *A*-subunit, which were also observed in saframycin B. The observation had been adumbrated by the FABMS/MS, with the *A*-and *B*-subunits together in the *m/z* 495 ion and the *C*-subunits in the *m/z* 224 and 250 ions (Figure 8). With ^{1}H-NMR information, protons of the *A*-subunit appeared to be identical with the unit in saframycin B while the chemical shifts of ^{13}C and ^{1}H-NMR signals were nearly identical (Ikeda *et al.*, 1983). Heteronuclear Multiple-Bond Correlation (HMBC) confirmed the *A*-subunit. The second aromatic unit (*B*-subunit) was also constructed and demonstrated to overlap the *A*-subunit as shown in Figure 9. From the basic fragments and correlation spectroscopy identified the *C*-subunit, and it could be combined to yield a complete structure for Et 743.

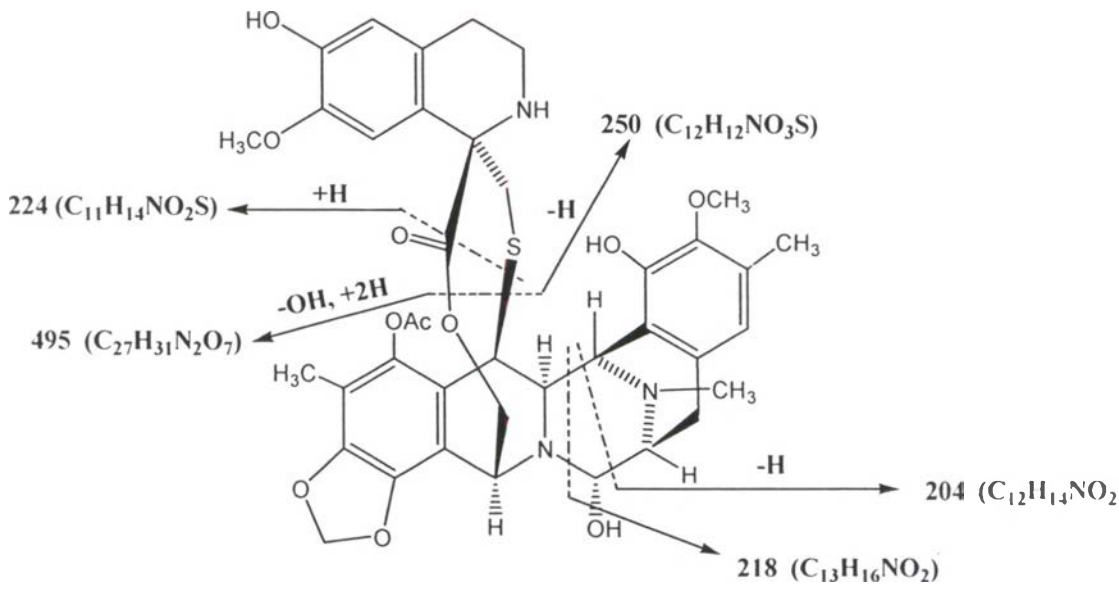

Figure 8. The partial fragmentation in FABMS of Et 743

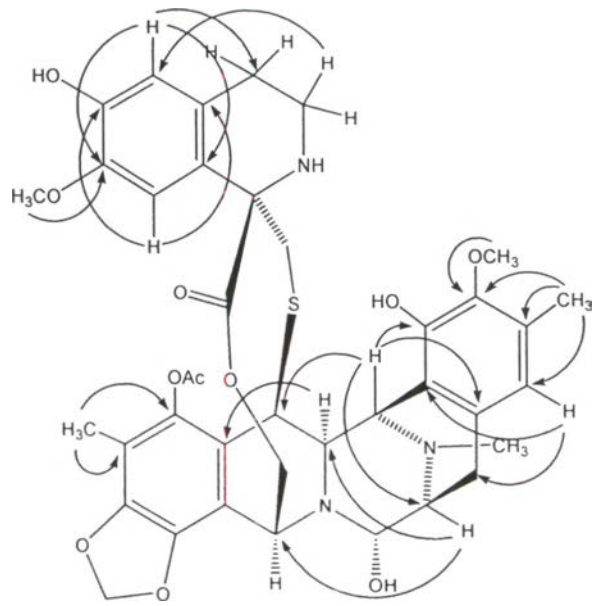

Figure 9. The partial long-range proton-carbon correlations in the HMBC spectra of Et 743

The structure of Et 743 and its relatives were ultimately confirmed by X-ray crystallography (Sakai *et al.*, 1992; Sainz-Diaz *et al.*, 2003). The chemical structures of ecteinascidins were unambiguously confirmed by the crystal structure of 21-*O*-methyl-N^{12}-formyl Et 729 and Et 734 N^{12}-oxide as shown in Figure 10. The molecular shape is highly compact and three large principal planar groups are observed in the three-dimensional structure of the Et 743 molecule, corresponding to three aromatic units which are nearly perpendicular to each other.

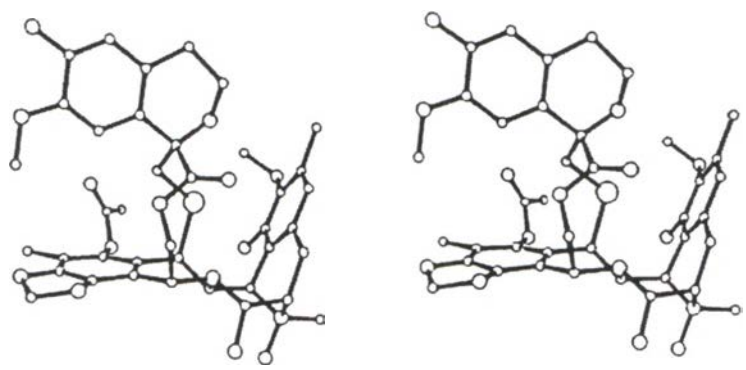

Figure 10. Stereoscopic X-ray crystallographic structure of 21-*O*-methyl-N^{12}-formyl Et 729 and Et 734 N^{12}-oxides

5. Synthetic studies of ecteinascidin

To date there have been three synthetic studies of Et 743. Corey *et al.* reported the first total synthesis of Et 743 in 1996. This strategy was followed by a semi-synthetic route from cyanosafracin B to Et 743 by Cuevas *et al.* in 2000. Lately, in 2002 another total synthesis route was reported by Fukuyama *et al.* Recently, Chen *et al.* and Zheng *et al.* independently accomplished total synthesis of Et 743 in 2006.

In 1996, Corey's group described the total synthetic route of Et 743 (Scheme 3) beginning from the α,β–unsaturated malonic ester **58**. It was subjected to selective allyl ester cleavage and stereospecifically Curtius rearrangement to form **59**, which was intramolecularly cyclized to afford the tetrahydroisoquinoline **62**. The combination of the building block **62** and **64** constructed the key monobridged pentacyclic intermediate **66**. The 10-membered lactone bridge was generated to produce carbamate intermediate **70**, which obtained the *N*-((allyloxy)carbonyl) functional group, **70** was subsequently converted to the α-keto lactone **71**, and then condensed with the phenylethylamine **72** to generate the spiro tetrahydroisoquinoline subunit. The reaction of **71** and **72** in the presence of silica gel generated the spiro tetrahydroisoquinoline stereospecifically which was then subjected to methoxymethyl (MOM) cleavage using trifluoroacetic acid in the presence of water and replacement of -CN by -OH to form Et 743.

Phthalascidin (Pt 650, **12**), one of analogs of Et 743, which has been found to exhibit cytotoxic activity essentially indistinguishable from that Et 743 (Martinez *et al.*, 1999). In 2000, Corey's group was successfully synthesized **12** based on the synthetic route of Et 743 (Martinez *et al.*, 2000) which was synthesized from the building blocks **62** and **64** *via* a common pentacyclic intermediate **67**, as shown in Scheme 4. The acetate **74** formed from the allyl ether **73**, finally transformed to **34**. Several other phthalascidin analogs were also prepared (Martinez *et al.*, 1999) as described in Scheme 5.

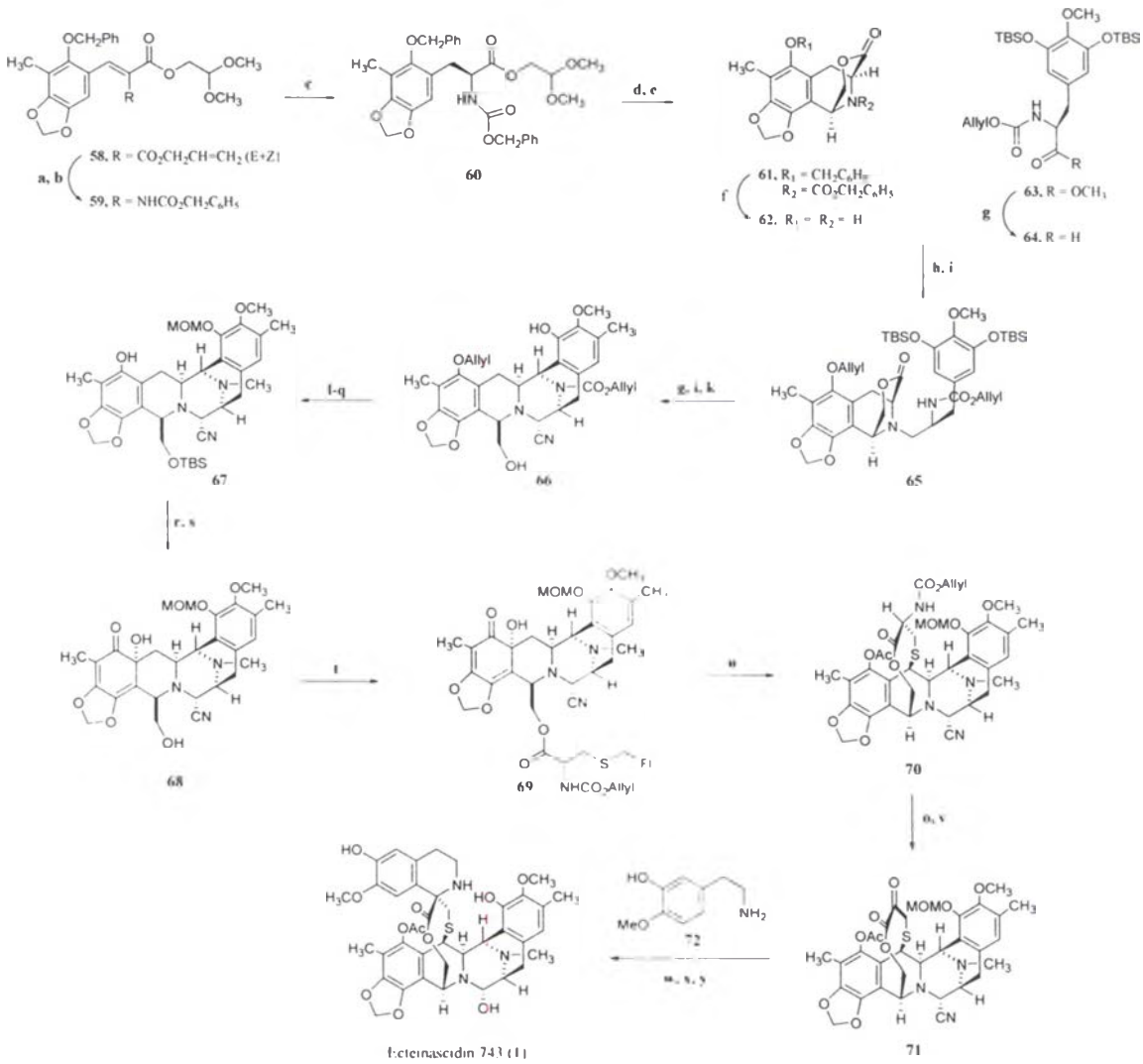

conditions: **a)** Et_3N-HCO_2H, $Pd(PPh_3)_4$; **b)** $(PhO)_2P(O)N_3$, Et_3N, 4 A^0 molecular sieves; 70 ^0C, BnOH; **c)** Rh[(COD)-(*R,R*)-DiPAMP]$^+BF_4^-$, 3 atm of H_2; **d)** BF_3OEt_2, H_2O; **e)** BF_3OEt_2, 4 A^0 molecular sieves; **f)** 10 % Pd/C, H_2; **g)** DIBAL, -78 ^0C; **h)** HOAc, KCN; **i)** Allyl bromide; Cs_2CO_3; **j)** KF·$2H_2O$; **k)** CH_3SO_3H, 3 A^0 molecular sieves; **l)** Tf_2NPh, Et_3N, DMAP; **m)** TBDPSCl, DMAP; **n)** MOMBr, *i*-Pr_2NEt; **o)** $PdCl_2(PPh_3)_2$, Bu_3SnH, HOAc; **p)** CH_2O, $NaBH_3CN$, HOAc; **q)** $PdCl_2(PPh_3)_2$, $SnMe_4$, LiCl, 80 ^0C; **r)** $(PhSeO)_2O$; **s)** TBAF; **t)** Alloc-Cys(CH_2Fl)-OH, EDC·HCl, DMAP; **u)** DMSO, Tf_2O, -40 ^0C; *i*-Pr_2NEt, 0 ^0C; *i*-BuOH, 0 ^0C; $(MeN)_2C$=N-*i*-Bu, 23 ^0C; Ac_2O, 23 ^0C; **v)** [N-methylpyridinium-4-carboxaldehyde]$^+T^-$, DBU, $(CO_2H)_2$; **w)** **72**, silica gel; **x)** CF_3CO_2H, H_2O; **y)** $AgNO_3$, H_2O.

Scheme 3. Corey's total synthesis of Et 743

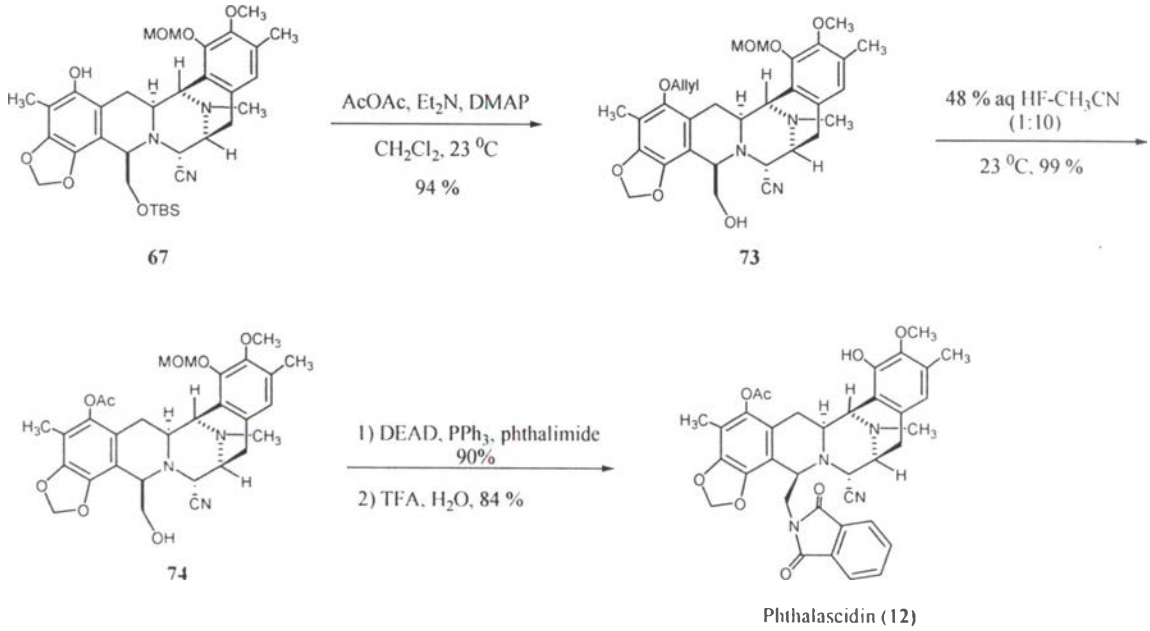

Scheme 4. Corey's synthesis of Phthalascidin-650

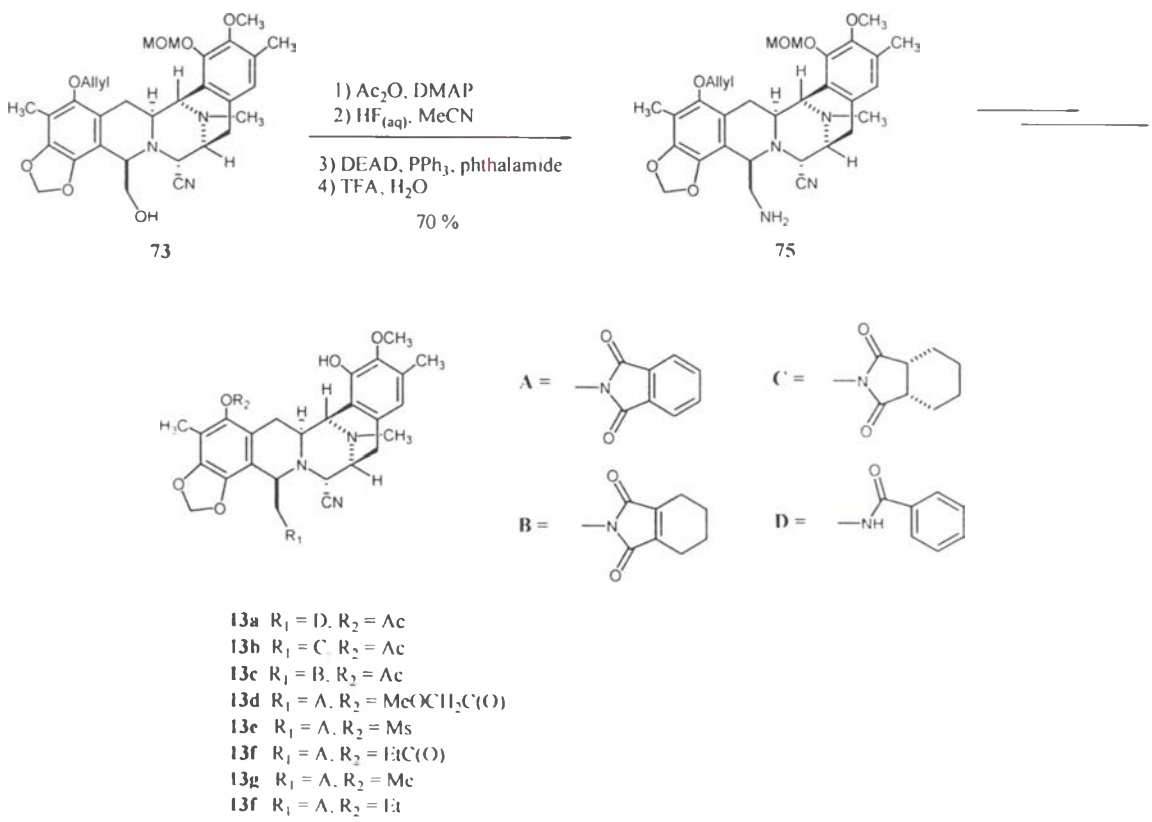

13a R_1 = D, R_2 = Ac
13b R_1 = C, R_2 = Ac
13c R_1 = B, R_2 = Ac
13d R_1 = A, R_2 = $MeOCH_2C(O)$
13e R_1 = A, R_2 = Ms
13f R_1 = A, R_2 = EtC(O)
13g R_1 = A, R_2 = Me
13f R_1 = A, R_2 = Et

Scheme 5. Preparation of Phthalascidin analogs

In 2000, Cuevas's group published a semi-synthetic route of Et 743 starting with cyanosafracin B **76**, which was available through fermentation of the bacterial *Pseudomonas fluorescens* (Ikeda *et al.*, 1983). Cyanosafracin B was converted into **77** *via* a four-step sequence and removal of the Boc group from **77** was followed by amide cleavage *via* an Edman degradation protocol providing **78**. The primary amine functionality was diazotized to alcohol **79**. By using of Corey's chemistry on similar substrate, a three-step sequence was used to form **80**. Dehydration under Swerm condition allowed the cyclization to afford **81**. Removal of the MOM and alloc protection groups was followed by ketone formation and the condensation with **72** in the presence of silica gel generated the spiro tetrahydroisoquinoline ring. Finally, the carbinolamine was transformed using Corey method to afford Et 743 (Scheme 6). The efficient synthetic of phathalascidin was also developed from the available cyanosafracin B which is outlined in Scheme 7. Acetylation of **77** was followed by cleavage of *N*-Boc and the Edman degradation of the alanine side chain afforded the free amino **82** which was allowed to react with phthalic anhydride and carbonyldiimidazole to give phthalascidin 650 (**12**).

In 2002, Fukuyama group described an efficient total synthesis route of Et 743 which would potentially lead to the development of a practical synthesis of this important compound and its analogs. The synthetic route started with the condensation of **83** and **84** into the diketopiperazine intermediate **86,** which was converted to the key intermediate **87** by four steps as shown in Scheme 8. The group succeeded in the formation **96** bearing the ten-membered sufide containing ring on the oxidation at the C-4 position of **93**. According to the protocol reported by Corey's group, biomimetic transformation reaction afforded the α-ketolactone, and subsequent Pictet-Spengler reaction with **72** afforded Et 770. Finally, generation of the labile hemiaminal from aminonitrile was effected by the well known method with silver nitrate in the mixture of acetonitrile and water to give Et 743 as described in Scheme 8.

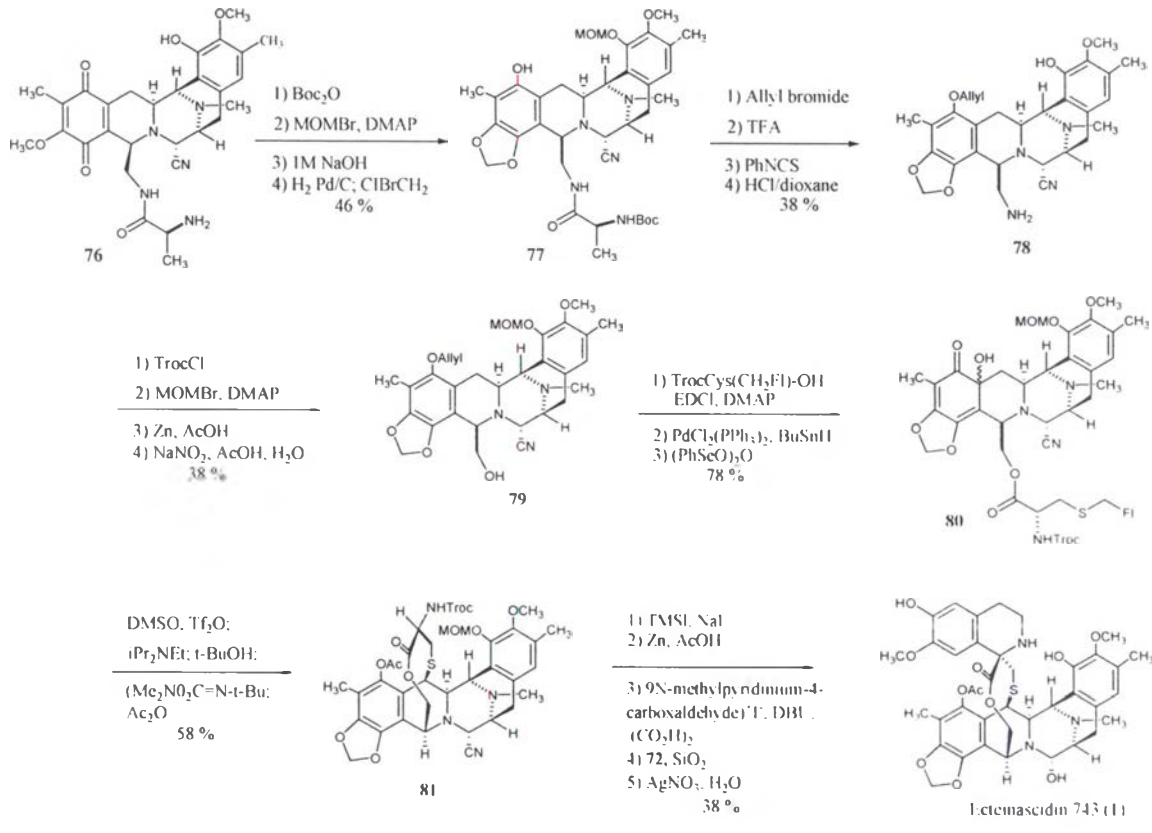

Scheme 6. Cuevas's semi-synthetic route of Et 743

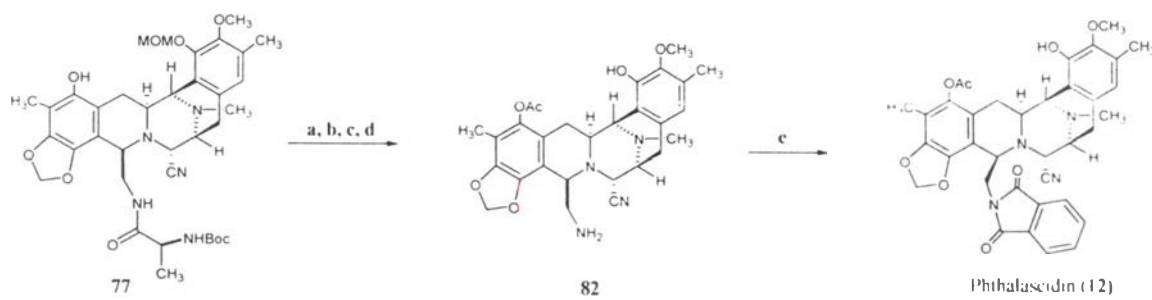

conditions: **a)** AcCl, pyridine, CH_2Cl_2, 0 ^{0}C; **b)** TFA, CH_2Cl_2, 23 ^{0}C, 60 %; **c)** Phenyl isothiocyanate, CH_2Cl_2, 23 ^{0}C, 63 %; **d)** HCl/dioxane 5.3 M, 23 ^{0}C, 87 %; **e)** Pht_2O, CDI, CH_2Cl_2, 23 ^{0}C, 93 %.

Scheme 7. Cuevas's synthetic route of Phthalascidin-650

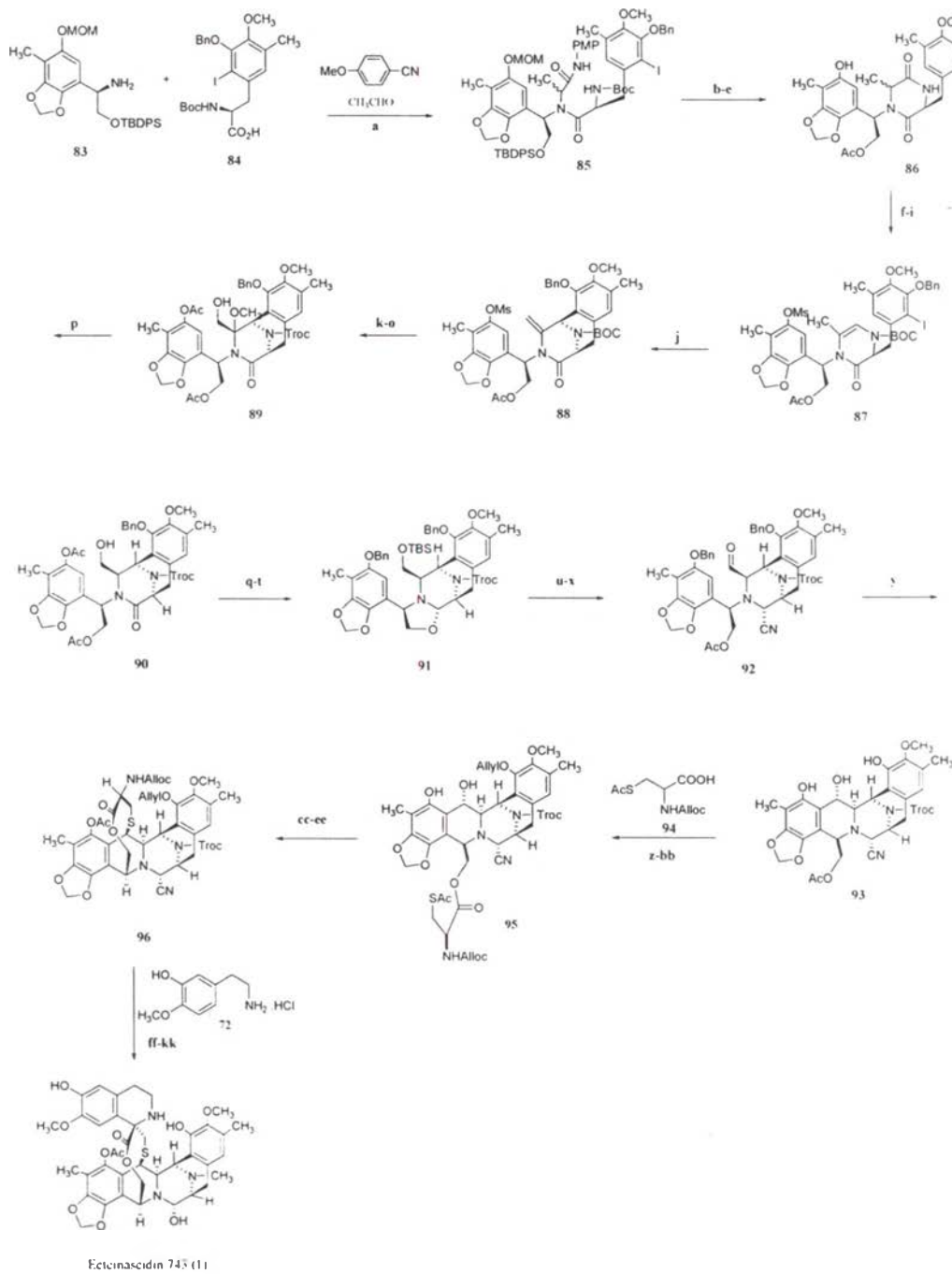

conditions: **a)** MeOH, reflux, 90%; **b)** TBAF, THF, rt, 89%. **c)** Ac_2O, pyridine, rt, 93 %; **d)** TFA, anisole, CH_2Cl_2, rt; **e)** EtOAc, reflus, 87%(2 steps). **f)** MsCl, Py, CH_2Cl_2, 0 °C, 91%; **g)** $(Boc)_2O$, DMAP, CH_3CN, rt, 97%; **h)** $NaBH_4$, H_2SO_4, EtOH-CH_2Cl_2, 0 °C; **i)** CSA, quinoline, toluene, reflux, 88%(2 steps); **j)** $Pd_2(dba)_3$, P(*o*-tol)$_3$, TEA, CH_3CN, reflux, 83%; **k)** NaOH, MeOH-H_2O, efflux; **l)** Ac_2O,pyridine, DMAP, rt, 93%(2 steps); **m)** TFA, CH_2Cl_2, rt; **n)** TrocCl, aq. $NaHCO_3$-CH_2Cl_2, rt, 74%(2 steps); **o)** dimethyldixane, MeOH-acetone, 0 °C, CSA, 90%; **p)** $NaBH_3CN$, TFA-THF, 0 °C, 94%; **q)** TBSCl, imidazole, DMF, rt, 92%; **r)** quanidinium nitrate, NaOMe, MeOH-CH_2Cl_2 , 0 °C, 85%. **s)** BnBr, K_2CO_3, CH_3CN, reflux, 91%; **t)** Red-Al, THF, 0 °C, 82%. **u)** TMSCN, BF_3-OEt_2, CH_2Cl_2, 0 °C, 73%; **v)** Ac_2O,pyridine, DMAP, rt, 92%; **w)** HF, CH_3CN, rt; **x)** Dess-Martin periodinane, CH_2Cl_2, rt, 92%; **y)** Pd/C, H_2, THF, rt, 84%; **y)** allyl bromide, *i*-Pr_2NEt, CH_2Cl_2, reflux, 89%; **aa)** K_2CO_3, MeOH, rt, 99%. **bb)** 103, WSCD HCl, DMAP, CH_2Cl_2, rt, 94%; **cc)** NH_2NH_2, CH_3CN, rt, 98%; **dd)** TFA, CF_3CH_2OH, rt; **ee)** Ac_2O,pyridine, DMAP, rt, 71%(2 steps); **ff)** Zn, AcOH, Et_2O, rt, 92%; **gg)** HCHO, AcOH, $NaBH_3CN$, MeOH, rt, 96%. **hh)** $Pd(PPh_3)_2Cl_2$, AcOH, *n*-Bu_3SnH, CH_2Cl_2, rt, 89%; %; **ii)** 4-formyl-1-methylpyridinium benzenesulfonate, DMF-CH_2Cl_2, rt, DBU, citric acid, 54%; %; **jj)** Amine, NaOAc, EtOH, rt, 96%; **y)** $AgNO_3$, CH_3CN-H_2O, rt, 93%.

Scheme 8. Fukuyama's total synthetic route of Et 743

6. Biological activity of ecteinascidins

In Vitro and In Vivo Activities

The ecteinascidins exhibits the most potent biological activities with significant margin relative to other tetrahydroisoquinoline antitumor antibiotics such as saframycin derivatives (Hill *et al.*, 1991; Rao *et al.*, 1992; Myers *et al.*, 2001; 2002; Tang *et al.*, 2003) and quinocarcin derivatives (Saito *et al.*, 1992), and also several clinically used anticancer agents such as adriamycin (DNA intercalator, DNA topoisomerase II inhibition), bleomycin (DNA cleaving agent through the oxygen radical species generation), camptothecin (DNA topoisomerase I inhibition), cisplatin (DNA alkylating agent), etoposide (DNA topoisomerase II inhibition), mitomycin C (DNA alkylating agent), and taxol (antimitotic agent causing microtubule stabilization) (Martinez *et al.*, 1999). Currently, Et 743 is investigation in Phase II/III in soft tissue sarcoma (Rinehart, 2000; Jimeno *et al.*, 2004; Henriquez *et al.*, 2005). To reach this status, it first showed *in vitro* activities against several common tumor cell lines, which were exceedingly high activities at low concentration as summarized in Table 2 and 3. *In vitro* studies exhibited a good tumor reduction for breast, melanoma, non-small cell lung cancer, and ovarian cancer as shown in Table 4. The activities of Et 743 was order of magnitude more potent than saframycin A against B 16 melanoma (Rinehart, 2000).

Table 2. The *in vitro* activity of Et 743 against several tumor cell lines

Tumor type	IC_{50} (nM)[a]
P388 (mouse leukemia)	0.34
L1210 (mouse leukemia)	0.66
A549 (lung cancer)	0.26
HT (colon cancer)	0.46
MEL-28 (melanoma)	0.50

[a]Pharma Mar, S.A., personal communication (Rinehart, 2000)

Table 3. The *in vitro* antitumor activity of Et 743

Cancer type	**LC_{50}** [a]
Colon	<1 pM
CNS	<1 pM
Melanoma	<1 pM
Renal	<1 pM
NSCL	4 pM
SCL	23 pM
Breast	<100 pM
Ovarian	2,020 pM
Prostate	3,430 pM
Leukemia	> 10,000 pM

[a] Data provided by Faircloth G, Jimeno J. Pharma Mar, S.A. (Rinehart, 2000)

Table 4. The *in vitro* activity of Et 743 against Human tumor Xenografted in Nude Mice[a]

Model	**Tumor type**	**Activity**	**T/C %**	**Tumor free (day)**
MX-1	Breast	9/10 CR(*)	<1	9/10(23) → 4/10(58)
MEXF989	Melanoma	6/6 CR	0.2	6/6 (35)
LXFL529	NSCLC	3/4 CR	0.1	3/7 (33)
HOC22	Ovarian	5/6 CR	<1	5/6 (120)
MRIH121	Renal	5/5 PR	30	-/5 (39)
PC2	Prostate	5/5 PR	44	-/5 (20)

[a] Data provided by Faircloth G, Jimeno J. Pharma Mar, S.A. (Rinehart, 2000)

In order to simplify and make up the stable molecule, other synthetic structurally related to ecteinascidin have been synthesized and tested for the biological activities. As shown in Table 5, several phthalascidin analogs were found to possess similar activities to that of Et 743 with regard to *in vitro* potency (Martinez *et al.*, 1999).

Table 5. Structure and antiproliferative of phathalascidin-related compounds

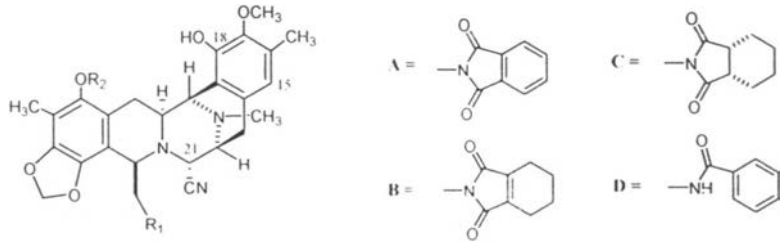

Analogs	R^1	R^2	Cell lines IC_{50} (nM)			
			A-549	HCT116	A357	PC-3
Pt 650 (12)	A	$CH_3C(O)$	0.95	0.38	0.17	0.55
13a	D	$CH_3C(O)$	3.2	0.59	0.35	0.64
13b	C	$CH_3C(O)$	1.5	0.85	0.27	1.1
13c	B	$CH_3C(O)$	1.2	0.61	0.35	0.75
13d	A	$CH_3OCH_2C(O)$	1.6	0.87	0.31	0.90
13e	A	$CH_3S(O)_2$	1.7	0.58	0.29	0.86
13f	A	$CH_3OCH_2C(O)$	2.1	1.2	0.51	2.9
13g	A	CH_3	3.1	1.4	0.55	3.1
13h	A	CH_3CH_2C	3.9	1.7	0.97	2.4
13i	C15-Chloro		2.8	1.0	0.35	1.1
13j	C15-, C18-*p*-quinone		1.7	0.80	0.45	0.68
13k	N12-[^{14}C]-CH_3		0.91	-	0.22	-
13l	C21-OH		1.0	0.61	0.20	0.53
13m	C21-H		2200	1100	610	850
13n	C18-OMOM		230	74	66	98
Et 743 (1)			1.0	0.50	0.15	0.70

In addition, phthalascidin also showed the greater activity than that of campothecin, etoposide and vincristine as shown in Table 6.

Table 6. Antiproliferative activity against mutant P388 of Et 743 and Pt 650

	Cell lines IC_{50} (nM)		
Drugs	**P388**	**Etopor-P388**	**Camptor-P388**
Et 743	0.12	0.24	0.30
Pt 650	0.19	0.18	0.21
Camptothecin	53	42	3.5×10^{4}
Etoposide	96	2.5×10^{3}	3.4×10^{2}
Vincristine	1.9	2.1	3.3

Mechanism of Action

The mode of action of ecteinascidins is complex, perhaps involving several mechanism as shown in Table 7. Ecteinascidin-DNA adduct appears to be reversible binding of the *A*-and *B*-subunits in the minor groove of DNA, with some differential effect by the *C*-subunit. It may or may not inhibit topoisomerase I and II, but Et 743 affects a good inhibition of RNA, DNA, and protein synthesis with the IC_{50} values of 8, 30, 100 nM respectively were also reported as shown in Table 8 (Rinehart, 2000).

Table 7. The mode of action of Et 743[a]

1. Effects on DNA:
   - Minor groove binder
   - Noncovalent binding to DNA
   - Sequence specificity (guanine rich areas
2. Effects on microtubules:
   - Not a tubulin inhibitor
   - Disorganizes assembly of microtubules
   - Time course for microtubule effects (1-8 h)

[a] Data provided by Faircloth G, Jimeno J. Pharma Mar, S.A.

Table 8. The *in vitro* biochemistry profile of Et 743[a]

Synthesis inhibition	IC_{50} *(nM)*
RNA	8
DNA	30
Protein	100
Polymerase inhibition	
RNA	100
DNA	2000
Topoisomerase inhibition	
Topo I	none
Topo II	none

[a] Data provided by Faircloth G, Jimeno J. Pharma Mar, S.A.

The mode of action was first reported in 1992 by Sakai *et al.* Interactions of ecteinascidins with DNA have been proposed on the basis of X-ray crystallography and the molecular modeling (Figure 11). It has been shown that the carbinolamine carbon (C-21) covalently bonded to N-2 of guanine base of the DNA chain. Mechanistically, within the physiological pH, the most basic N-12 at *A*-subunit would be protonated. In close proximity of 2.5 Å, the hydroxyl group at C-21 would then be protonated, while the electron pair of N2 of *B*-subunit would catalyze the dehydration to result the reactive iminium intermediate, which subsequently reacts with DNA through the exocyclic 2-amino group of guanine in the duplex DNA as shown in Scheme 9 (Moore *et al.*, 1998). It is probable that the water remains hydrogen bonding at this point in the mechanism. Later, the investigation revealed that DNA adduct was modified with the homopolymeric oligonucleotide dG/dC, while neither the dI/dC nor the dA/dT oligonucleotide were (Pommier *et al.*, 1996), and the alkylation was best in GC-rich regions (Zewail-Foote *et al.*, 1999, 2001; Marco *et al.*, 2002). Remarkably, the alkylation is DNA sequence specific with guanine, and reverse on DNA denaturation (Era *et al.*, 2001). These characteristics of Et 743 apart from other DNA alkylating agent currently used in cancer chemotherapy, which was a unique mechanism of Et 743 (D'Incalci *et al.*, 2002).

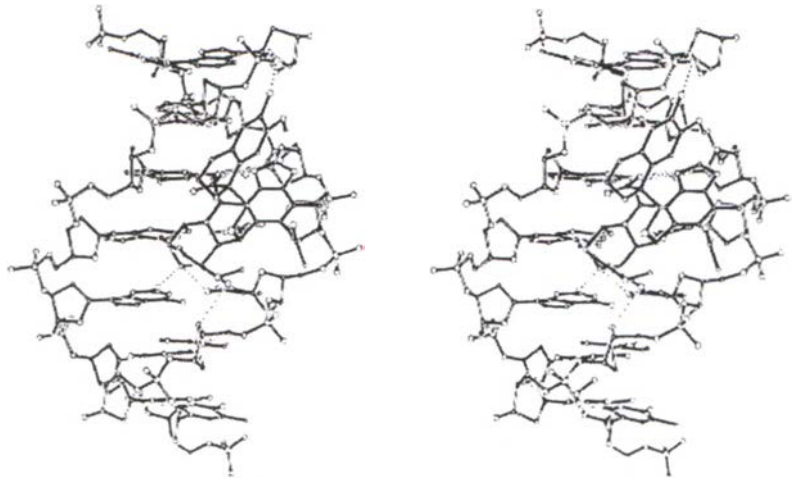

Figure 11. A model of the Et-DNA adduct produced by a computer modeling study (The DNA sequence is d(TTGGGAA), with the middle G as the target base for the alkylation reaction of Et)

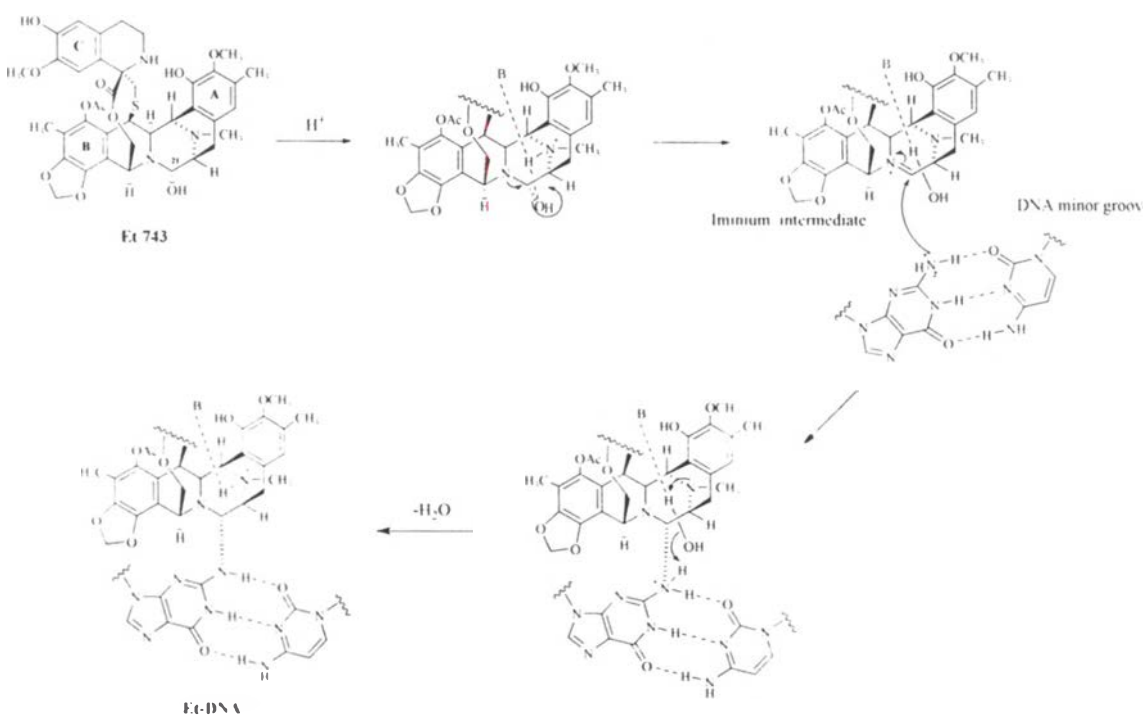

Scheme 9. The proposed mechanism reaction of an iminium intermediate with the guanine 2-amino group.

In comparison, the other α-carbinolamine-containing antibiotics also alkylated N-2 of guanine, however the ecteinascidins are the wedge-shaped, while either saframycin and naphthylidinomycin are in planar-shaped. The wedge-shaped is due to the *C*-subunit, which imparts rigidity to the ecteinascidin molecule and for covalent adduct formation forces the minor groove to widen and concomitantly bends DNA into the major groove (Zewail-Foote and Hurley; 1999). The NMR data base on model of Et 743 binding to duplex DNA, $[d(CGTAAGCTTACG)]_2$), indicating that the *A*-subunit is perpendicular to the helical axis and oriented to allow a hydrogen bond between 18OH and 21TO1', and also the protonated 12NMe showed hydrogen bond to 21TO2 and 21TO1'. Also the 6Me, 5OAc, H23, H4, and H11 protons at the *B*-subunit exhibited hydrogen bond to 18G, 19C, 20T, and 21T respectively (Figure 12) (Moore *et al.*, 1997). While, 7'OMe at the *C*-subunit displayed a weak NOE signal to 8TH3', suggested that the *C*-subunit is perpendicularly projected above the minor groove. These observation suggested that *A*- and *B*-subunits and the carbinolamine on ecteinascidin molecule appear to be the critical structural features responsible for DNA recognition and bonding, while the *C*-subunit centrally protrude from the minor groove. In summary, the covalent attachment of Et 743 to DNA and flanking donor/acceptor hydrogen bond of DNA accelerate a locally widened minor groove of DNA, which also has an extra-helical protrusion in an otherwise bent DNA.

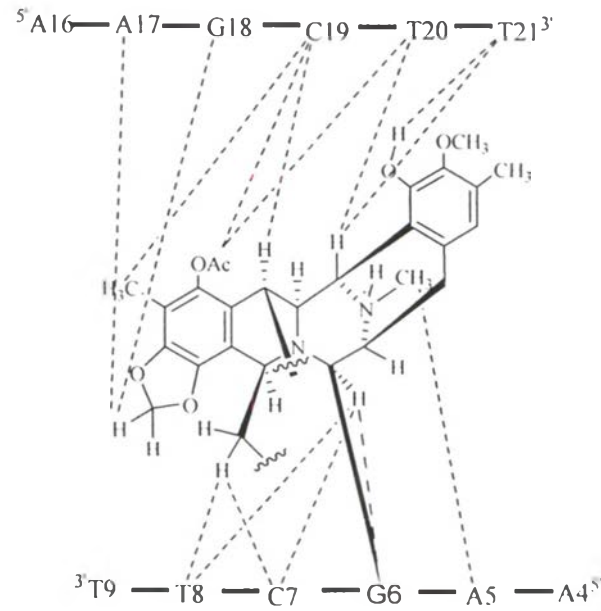

Figure 12. Partial model of Et-743 bound to the 12-mer oligonucleotide.

Pommier's group reported the unique mechanism of Et 743 that it halted the nucleotide-excision repair (NER) system in cell (Takebayashi *et al.*, 2001). This DNA cleavage would then lead to death of the cell. Hurley group also reported the effect of Et 743 upon the NER mechanism (Zewail-Foote *et al.*, 2001). It was described that the DNA covalent adduct trapped on intermediated in NER processing which would not allowed the DNA to be fully repaired. Incubation of the bacterial multisubunit endonuclease UvrABC with DNA that was treated with Et 743 showed that the DNA-Et 743 adduct was recognized and incised. The incision was inhibited at high Et 743 concentration. It was noted that the incision frequency was sequence related with the stability of DNA-Et 743 adduct. Era *et al.* (2001) reported the effects of 1 hour of Et 743 exposure, evaluated by a BrdUrd/DNA biparametric flow-cytometric analysis, showed that cell in the S phase during drug treatment progressed through this phase of the cell cycle more slowly than control cell. In addition, cell that were in the G_1 phase progressed through the S phase slowly. At 24 hours, a high percentage of Et 743 treated cells were arrested in the G_2 phase, and only 120 or 180 hours afterward, progressed to mitosis and restarted a new cell cycle. By the synchronizing colon cancer SW620 cells, the sensitivity to Et 743 was comparatively evaluated in cell in G_1 S and G_2-M phase. The results showed that the highest sensitivity to the drug occurred when were in G_1, and the lowest occurred when cells were in G_2-M phase. This indicating that the interaction between Et 743 and DNA is preferentially effective in S phase cells. Also this group described that Et 743 induces significant increase in p53 level, which promotes apoptosis in cell lines expressing wild-type p53. The findings that G_1 phase cells are hypersensitivity and that NER-deficient cells are resistant to Et 743 indicate that the mode of action of Et 743 is unique features and different from that of DNA-interacting drugs.

Clinical investigation

Because of the unique features, Et 743 was taken into clinical development, and activity in soft tissue sarcoma was suggested even in the phase I studies. The phase I program with Et 743 in adult patients has including six phase I trials, five in adults and one in pediatric patients, investigating different schedules (Rinehart, 2000; Ryan *et al.*, 2001; Villalona-Calero *et al.*, 2002; Twelves *et al.*, 2003). At the dose-limiting toxicities, Et 743 was generally tolerated with non-cummulative haenmatological (thrombo-cytopenia and neutropenia) and hepatic toxicities (elevation of transaminases) being the most commonly reported side effects. The most severe adverse effects, encountered in less than 2% of patients, were long-lasting pancytopenia, renal and hepatic failure and rhabdomyolysis. Evidence of objective activity, including long-lasting responses, was observed in sarcoma, breast cancer, ovarian cancer, and mesothelioma. In addition, Et 743 showed activity in crease of advanced sarcoma that had relapse or were resistant to conventional therapy. These observations, established a solid foundation to further investigate the activity of Et 743 in connective tissue tumors. The recommended dose and schedule has been established as 1,500 $\mu g/m^2$ of Et 743 administered as a continuous intravenous (i.v.) infusion over 24 hours. In June 2001, the European Agency for the Evaluation of Medicinal Products (EMEA) awarded Et 743 (Yondelis™, Trabectedin™ are namely) "*orphan drug*" status for treatment of soft tissue sarcoma (STS) (Garci'a-Fern'andez *et al.*, 2002).

The phase II trials have studied in several indications, including STS, breast, ovarian, endometrium and lung cancer (Schwartsmann *et al.*, 2001; Jimeno *et al.*, 2006). Results from three multicentre phase II clinical trials performed in Europe and US on a subset of pre-treated or chemo-naive patients with metastatic STS, showed the following as median time to disease progression of 2.8 months, median overall survival (OS) time 10.2 months, 1-year OS rate of 40% and 6-months progression free survival (PFS) rate of 27.2%. Tumor response, partial and minor, or stable disease was reported in 57% of patients, with evidence of long lasting (median duration responses 17 months) tumor control (Le Cesne *et al.*, 2001; PharmaMar Annual report, 2002). In addition, Pharma Mar has investigated the effects of combination of Et 743 with cisplatin, paclitaxel or

doxorubicin to results that the combination of Et 743 with cisplatin showed more than additive effects in several preclinical systems and initial clinical results appeared to confirm the preclinical findings (D'Incalci *et al.*, 2003). Preliminary data reported from phase II studies in advanced breast and ovarian cancers also suggested activity against these tumor (Ryan *et al.*,2002) and five clinical studies of Et 743 were also presented by Pharma Mar in partnership with Johnson & Johnson Pharmaceutical Research & Development, L.C.C. (J & JPRD) (PharmaMar news release, 16-05-2005).

The phase III pivotal study in ovarian cancer comparing the combination of Et 743 plus doxil to doxil alone is ongoing to demonstrate that Et 743 plus doxil is superior to doxil as a single agent, in second line in the treatment of patients with ovarian cancer (PharmaMar news release, 04-04-2005).

7. *N*-demethylation of the ABC ring model compounds

The most relevant structural difference of Et 729 (**5**) with other members of the ecteinascidin family is the absence of 12-*N*-methyl group in the bridgehead nitrogen of the fused tetrahydroisoquinoline unit. Et 736 (**10**) and Et 722 (**11**) are respectively related to those of the **1** and **5** series, but their tetrahydro-β-carboline unit presumably come from tryptamine instead of dopamine as shown in Scheme 2 and the chemical structure shown in Figure 13. Compounds **11** and **12** were also found to have high *in vitro* activities against L1210 with IC_{90} of 2.5 and 5.0 ng/ml, respectively (Sakai *et al.*, 1992). Et 722 was also highly active *in vivo* against variety of cell lines (Table 9). In the case of Et 729, which exhibited higher *in vivo* activities against P 388 leukemia than Ets 743 and 745 (Table 10).

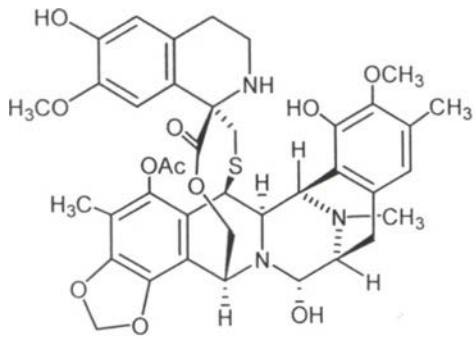

Et 743 (1)

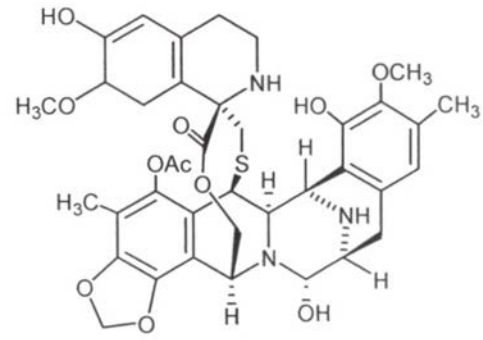

Et 729 (5)

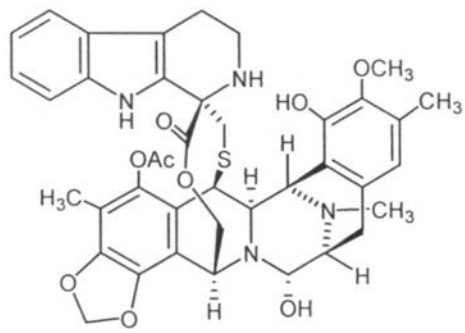

Et 736 (10)

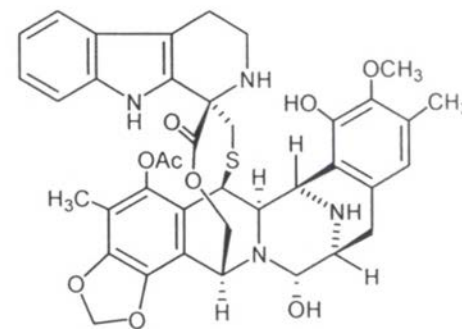

Et 722 (11)

Figure 13. Structures of Ets 743, 729, 736 and 722

Table 9. The activity of Et 722 against several tumor cell lines

Tumor type	dose (μg/kg)	T/C[a]
P 388 leukemia	25	>265
B 16 melanoma	50	200
Lewis lung carcinoma	50	0.27
LX-1 lung carcinoma	75	0.00

[a] T/C = is the increased lifespan of mice treated with the drug versus the control group (Rinehart, 2000)

Table 10. The activity of Ets 729, 743, and 745 against P 388 leukemia

compounds	dose (μg/kg)	T/C[a]
Et 729	3.8	214
Et 743	15	167
Et 745	250	111

[a] T/C = is the increased lifespan of mice treated with the drug versus the control group (Rinehart, 2000)

Therefore, the synthesis of Et 729 requires demethylation reaction of the bridgehead nitrogen. In 2003, Cuevas group reported the successful synthesis of Et 729, which a demethylation of *N*-methyl intermediate was carried out by Polonovsky reaction with *m*-chloroperbenzoic acid (*m*-CPBA) (Menchaca *et al.*, 2003). According Scheme 10, silylation of the primary alcohol of intermediate **97** under standard condition ***a*** and protection of the phenol with (2-methoxyethoxy) methyl (MEM) furnished **99**. The attempts demethylation in CH_2Cl_2 with *m*-CPBA, TEA, and TFAA (Frohlic *et al.*, 1998) afforded the key intermediate **100** in high yield (85 %). However, the critical *N*-demethylation of the tertiary amine under different conditions described such as I_2/CaO, vinyl chloroformate, *tert*-butylhydroperoxide/$RuCl_2(PPh_3)_2$, or $RuCl_3/H_2O_2$ led to undesired products or unaltered starting material. With compound **100**, deprotection of the allyl group, oxidation of phenol group, and subsequent protecting with allyl bromide of the bridgehead amine furnished **103**, which was submitted to desilylation to give **104**. The esterification of the resulting alcohol with (*R*)-*N*-[(*tert*-butoxy)carbonyl-*S*-(9-fluorenylmethyl)]cysteine and subsequent cyclization gave the ten-membered lactone bridge intermediate **106** *via* formation of the exo quinone methide followed by nucleophilic addition of the phenoxide ion. Simultaneous removal of the *t*-butoxy-carbonyl (Boc) and MEM protecting group afforded **107**. Next, transamination and introduction of the dopamine moiety by Pictet-Spengler reaction gave intermediate **109**. Deprotection of the allyl protecting group and replacement of -CN by -OH with $AgNO_3$ gave Et 729 (**5**) in 42 % yield.

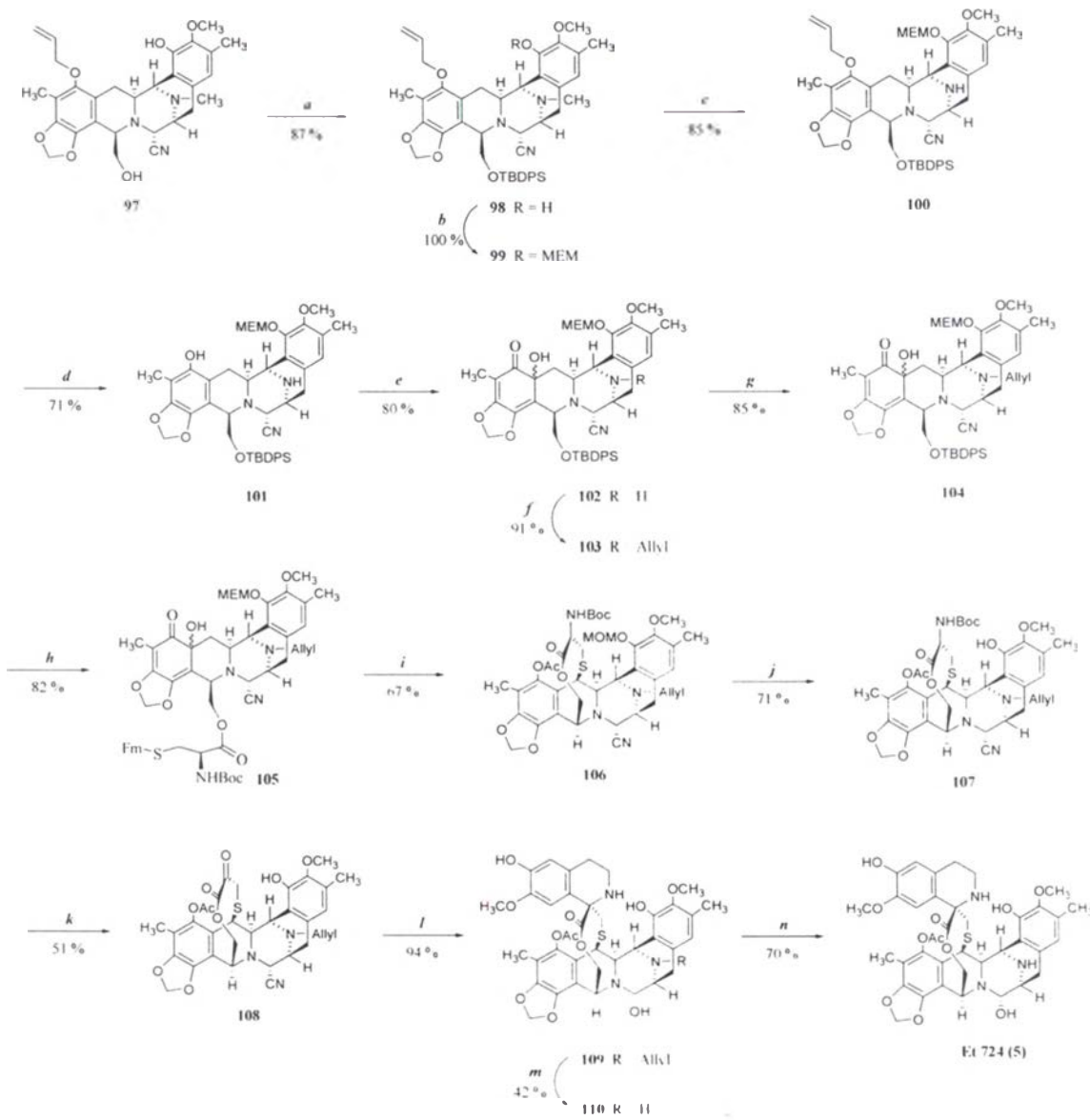

conditions: **a)** TBDPSCl, imidazole, DMAP, DMF; **b)** MEMCl, NaH, THF; **c)** MEMCl, TEA, TFAA, CH_2Cl_2; **d)** $HSnBu_3$, AcOH, $PdCl_2(PPh_3)_2$, CH_2Cl_2; **e)** $(PhSeO)_2O$; **s)**, CH_2Cl_2; **f)** Allyl bromide; Cs_2CO_3, DMF; **g)** TBAF, THF; **h)** L-cysteine, EDC-HCl, DMAP, DIPEA, CH_2Cl_2; **i)** DMSO, Tf_2O, *t*-BuOH, *tert*-butyltetramethyl guanidine, Ac_2O, CH_2Cl_2; **j)** *p*-TsOH, $CHCl_3$; **k)** *N*-methyl pyridinium-4-carboxaldehyde iodide, DBU, oxalic acid; **l)** 3-hydroxy-4-methoxyphenylethylamine, silica gel, EtOH; **m)** $HSnBu_3$, AcOH, $PdCl_2(PPh_3)_2$, CH_2Cl_2; **n)** $AgNO_3$, H_2O-CH_3CN

Scheme 10. Synthetic pathway of Et 729

Murahashi et al, described the oxdative *N*-demethylation of amines using the ruthenium-catalyzed reaction of **111** with *tert*-butyl hydroperoxide afforded the corresponding α-(*tert*-butyl-dioxy) alkylamines **112**, subsequent acid treated furnished yielding of the demethylation product **113**. (Scheme 11, **a**) (Murahashi *et al.*, 1988). In the other hand, the ruthenium-catalyzed oxidation was carried out in hydrogen peroxide in the presence of methanol also resulted the *N*-demethylation product (Scheme 11.**b**) (Murahashi *et al.*, 1992). Other condition, the reaction of methyl chloroformate and hydrazine (Csutoras *et al.*, 2004) with 3-deoxymorphine **115** can be reacted to afford the demethylation product **116** while **117** was also obtained as a side product (Scheme 12).

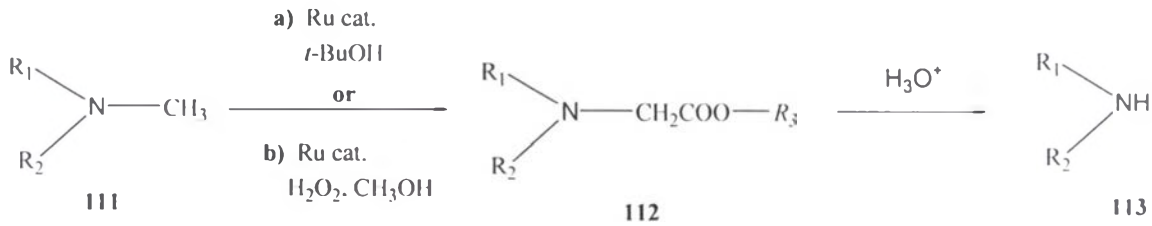

Scheme 11. The oxdative *N*-demethylation of amines using the ruthenium-catalyzed reaction with **a**) *tert*-butyl hydroperoxide, **b**) hydrogen peroxide

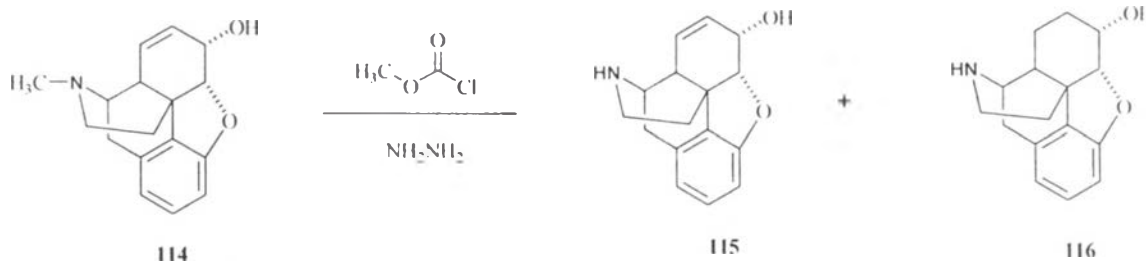

Scheme 12. The oxdative *N*-demethylation of amines methyl chloroformate and hydrazine

With structurally point of view, the core structures of ecteinascidin and its related compounds are characterized by a bis-tetrahydroisoquinoline pentacyclic system, ABCDE rings (**117**) (Tang *et al.*, 2003; Chan *et al.*, 2005), which is believed to be the primary pharmacophore through the preliminary structure activity study of Et 743 and its analogs. In order to reduce the number of steps for synthesis and simplified the structure of ecteinascidin or its related compounds, the structural model bearing the ABC ring system **44** were synthesized (Figure 14).

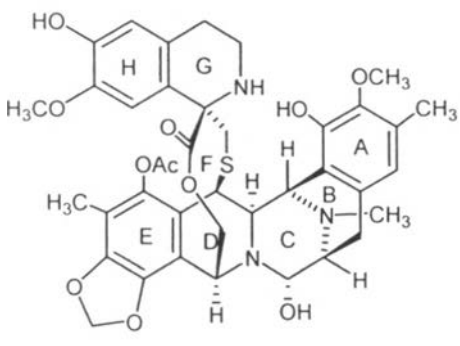

Ecteeinascidin 743 (**1**)

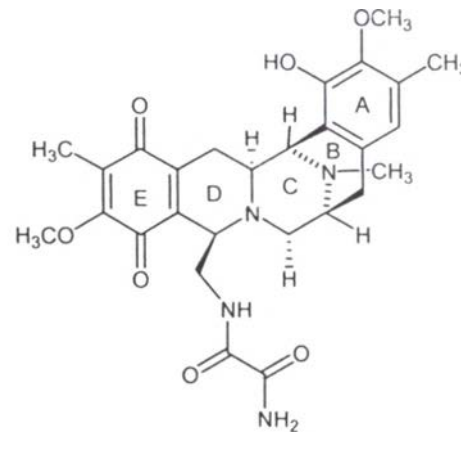

Safracin A

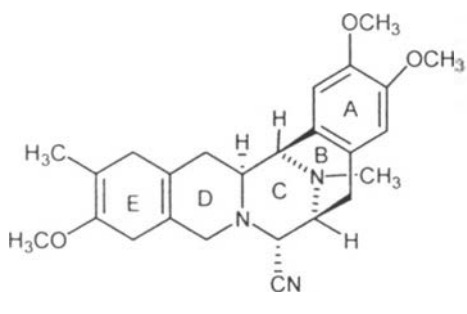

117

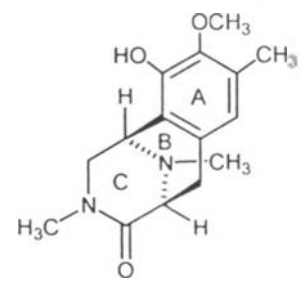

44

Figure 14. Structures of Et 743, Safracin B and the ABC ring model of ecteinascidins

In 1992, Kubo group reported the synthetic strategy for the model of ABC ring system of safracins. The condensation between 1,4-diacetyl-2,5-piperazinedione (**118**) and 4-methoxy-3-methylbenzaldehyde (**119**) yielded 3-arylidene-2,5-piperazinedione (**120**), which was further subjected to series of 14 steps of reaction and furnished the model compound **44** in 5 % yield (Scheme 13) (Saito *et al.*, 1992). Lately, in 2000, the improved synthesis of ABC ring model *via* the useful intermediate **129** was reported. The synthetic pathway started from the reaction of available **118** and benzaldehyde derivative **121**, which was prepared for seven steps of reaction starting with 2,3-dihydoxytoluene. Then, the result was reacted as followed previously method to afford the intermediate **129**, meanwhile the conversion of **127** into the intermediate **129** via the benzaldehyde derivatives **128** was also studied (Scheme 14). Then the intermediated **129** was cyclized to yield the cyclic compound, which was transformed through several steps to afford the high yield (95 %) of **44** as described in scheme 15 (Saito *et al.*,2000). Herein, the demethylation of *N*-methyl group of ecteinascidin molecule will be worked on the model compound prior and the twelve model compounds will be used. The chemical structures of the model compounds are summarized in Figure 3.

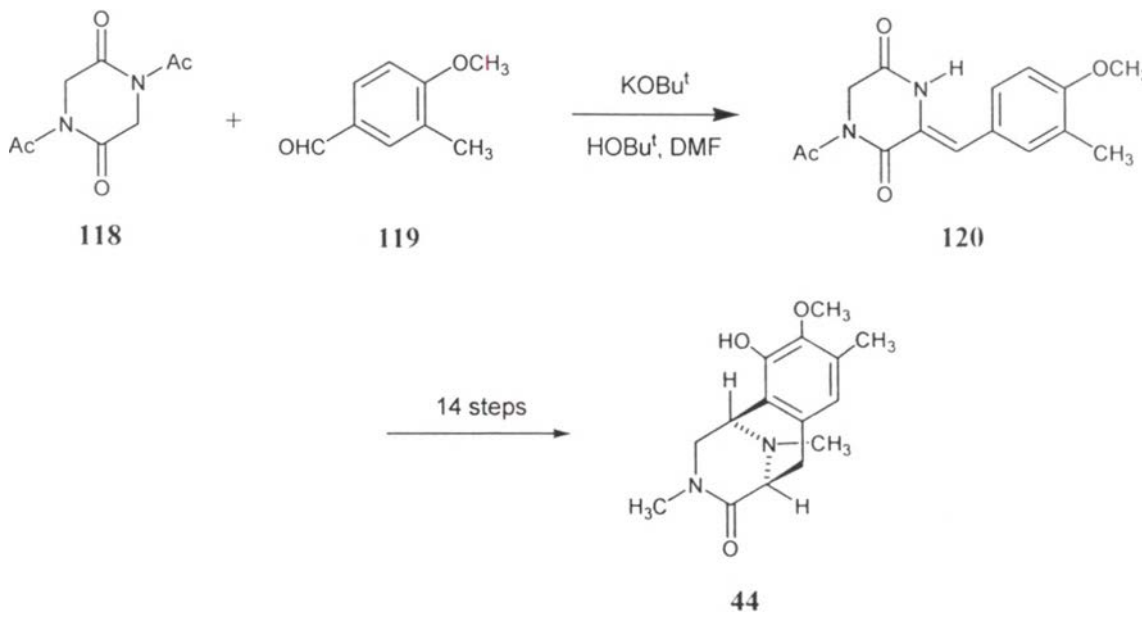

Scheme 13. Kubo's synthesis of the ABC ring model of ecteinascidins

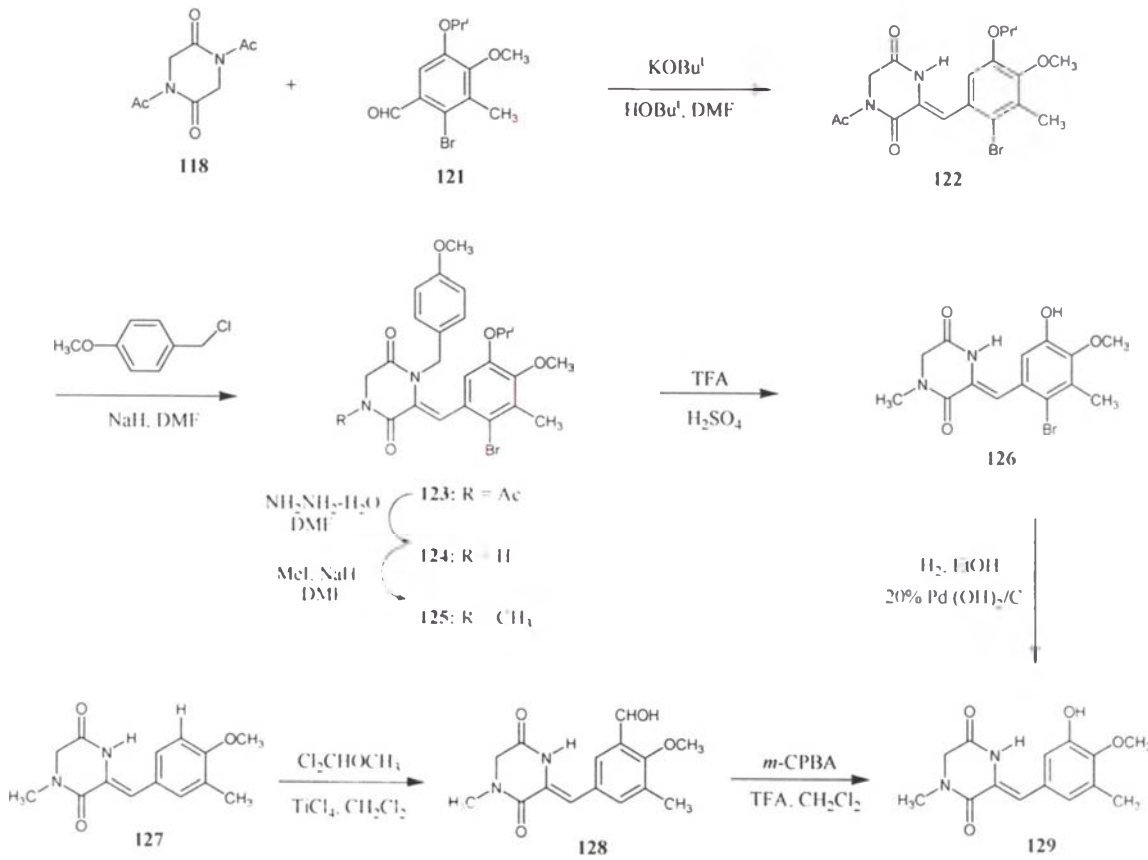

Scheme 14. Synthetic route of the useful intermediate **129**

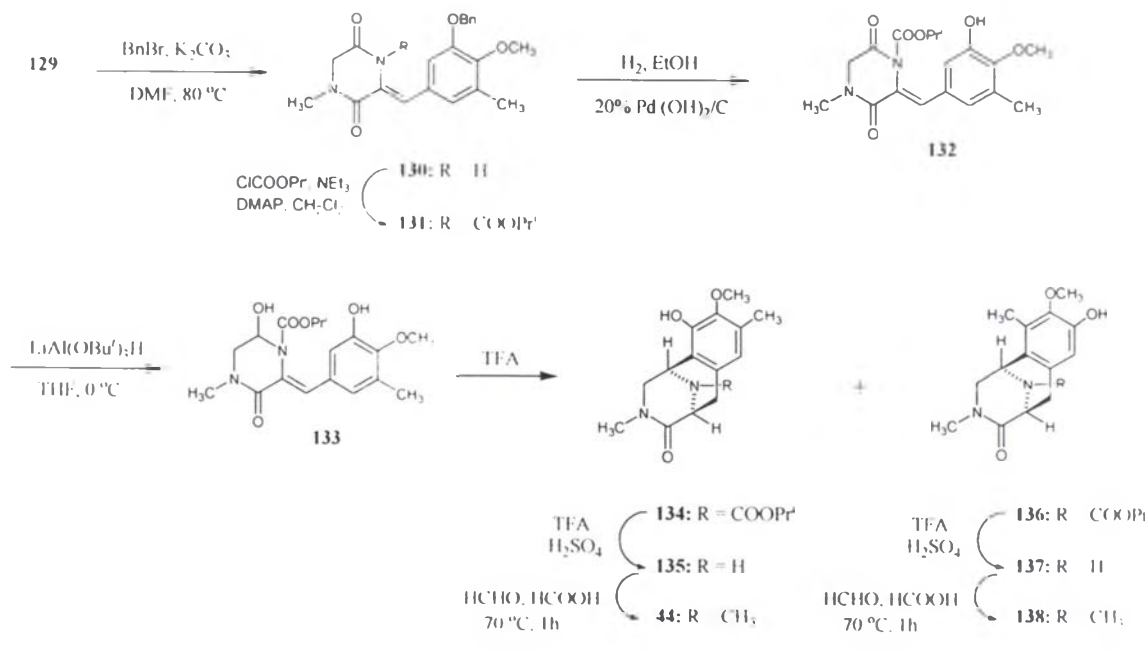

Scheme 15. Practical synthetic of the ABC ring models of ecteinascidins